COMPLETE PROPAGATION MODEL STRUCTURE INSIDE TUNNELS

Ke Guan¹, Zhangdui Zhong¹, Bo Ai¹, *, Ruisi He¹, Binghao Chen¹, Yuanxuan Li¹, and Cesar Briso-Rodríguez²

¹State Key Laboratory of Rail Traffic Control and Safety, Beijing Jiaotong University, Beijing 100044, China

²Escuela Universitaria de Ingeniería Técnica de Telecomunicación, Universidad Politécnica de Madrid, Madrid 28031, Spain

Abstract—In this paper, a complete model structure for propagation inside tunnels is presented by following the segmentation-based modeling thought. According to the concrete propagation mechanism, totally five zones and four dividing points are modeled to constitute three channel structures corresponding to large-size users and small-size users. Firstly, the propagation characteristics and mechanisms in all the zones are modeled. Then, from the view point of the propagation mechanism, the criterion of judging the type of a user is analytically derived. Afterwards, all the dividing points are analytically localized as well. Finally, a panorama covering all the propagation mechanisms, characteristics, models, and dividing pints for all types of users is presented for the first time. This panorama is very useful to gain a comprehensive understanding of the propagation inside tunnels. Validations show that by using the analytical equations in this paper, designers can easily realize a fast network planning for all types of users in various tunnels at different frequencies.

1. INTRODUCTION

To give the answer to the developing demand for high-performance wireless communication systems inside tunnels, many investigators have performed simulations and measurements of wave propagation in the last four decades. Based on different methods, such as vector parabolic equation (VPE) [1], geometrical optics (GO) [2, 3], modal analysis [4–6], finite-difference time-domain (FDTD) [7–9], etc.,

more and more researchers are inclined to analyze the propagation characteristics by separating various zones along the tunnel. This segmentation-based thought is gradually formed but still lacking in unanimous consensus on the zone division and corresponding propagation mechanism modeling in each zone.

In general, to describe the propagation inside tunnels, a large number of models are presented in a two-slope curve (e.g., in [4]) that the losses are described by two different expressions. In these models, the dividing point (also known as the break point [10]) between two slopes separates the whole process into two segments. Before the break point is the near region, where the high order modes are dominant; waveguide effect has not been established, and therefore, the signal undergoes larger loss and stronger fluctuations. After the break point is the far region, where the high-order modes have been greatly attenuated; the fundamental modes guide the propagation so that the wave suffers smaller loss and slight fading.

Table 1. Propagation mechanisms in the near region and the far region (from the classical publications).

	Near Region	Far Region
Propagation Mechanism	Free Space Propagation [11]	Basic Mode Waveguide [10–12]
	Multi-Mode Waveguide [10]	Free Space Propagation [12]
	Near Shadowing Phenomenon [13]	

In term of the propagation mechanisms in the near region and the far region, there is a wide gap between different academic views. As shown in Table 1, at least three propagation mechanisms in the near region and two propagation mechanisms in the far region have been presented by various classic publications [10–13]. All these references justified their own claims but hardly refuted the conflicting standpoints. This leads to confusion in the network planning for the communication systems inside tunnels, as the choice of different mechanisms results in different losses. However, we still can get the following inspirations from such a chaotic situation:

- One propagation zone should only contain one mechanism, otherwise it should be spitted into two or more zones according to how many propagation mechanisms are discovered in it. Hence, the classic two-slope structure, only the near region and the far region, is not sufficient to cover all the propagation mechanisms, new zones are required to supplement.

- The essence of the near shadowing phenomenon [13] is that the line of sight (LOS) or the first Fresnel zone between transmitter (Tx)

and receiver (Rx) is (partially) blocked by the user itself. This is why such effect is clearly observed in the cases when the user is relatively large, such as long trains in subway tunnel [13, 15], but does not appear in the cases when the user is very small compared with the tunnel. Thus, the relation between the size of the user and the size of the tunnel should be considered.

- In order to determine the range of each propagation mechanism, locations of all the dividing points should be accurately modeled. Otherwise the whole network planning solution will still be wrong even though the propagation loss in each zone is modeled correctly.

By following these inspirations, a complete model structure is presented. Following are the main contributions of this paper:

- Present a complete structure that interprets all the propagation mechanisms by dividing the whole process into various zones, refining and extending existing segmentation-based models.
- Model the propagation loss in every zone by integrating the advantages of different modeling techniques.
- Analytically localize the dividing points between every adjacent zones, which is very useful for quick estimation
- Support inspirational discussions for understanding the philosophy and application of the segmentation-based modeling thought.
- The complete model structure helps to unify clashing perspectives, establish a comprehensive understanding of the propagation inside tunnels, and predict the coverage in complex tunnel environments.

2. COMPLETE PROPAGATION MODEL STRUCTURE

Based on the change law of the propagation mechanisms inside tunnels, a complete structure is presented for the first time. It embodies the segmentation-based thought that divides the whole process into different regions and employs proper techniques in each segment. The structure consists of five propagation zones, namely: the free space propagation zone, the near shadowing zone, the multi-mode propagation zone, the fundamental model propagation zone, and the extreme far zone. As shown in Fig. 1, the complete structure is more comprehensive than the previous models:

- Compared with the two-slope model structure [4, 10], the new structure subdivides the near region into the free space propagation zone and the multi-mode propagation zone, and adds the extreme far zone. This clarifies the mechanism constitution
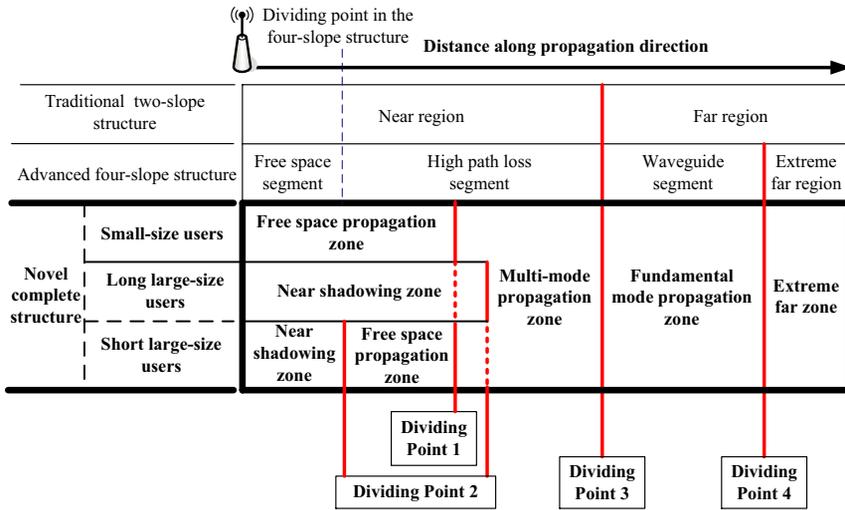
Figure 1. Complete propagation model structure in tunnels.

in the near region, and reveals the fact that the waveguide effect vanishes at extreme distances.

- Compared with the advanced four-slope structure [12] that utilizes the free space model to localize the dividing point, the novel one concerns the generality of the algorithm for localization of the dividing points, and derives general models for all the dividing points inside arbitrary cross-sectional tunnels.

- By introducing the near shadowing zone, the size of the user is fully considered. Finally, depending on the relations between sizes of users and tunnels, totally three situations constitute the complete structure. All the propagation characteristics and the locations of all the dividing points are modeled by analytical formulas, so that the complete structure can be easily implemented for the network planning in any concrete situation.

Normally, a single modeling technique is sensitive to certain propagation mechanisms or characteristics. Since the propagation inside tunnels includes various mechanisms, a hybrid model extending and integrating advantages of various methods is presented:

- Theoretical models are based on simplified or ideal environments, so they are easy to be implemented but not sensitive to the fading resulting from the real environments. Since the fluctuations of the signal in the free space propagation zone and the extreme far zone are slight, the propagation loss is the most important metric and can be derived by the theoretical free space model.

- Empirical models offer the first-hand information from measurements, but the physical meaning is not sufficient. In the near shadowing zone, the final effect (of the combination of the shadowing effect owing to the large-size user and the multi-path propagation resulting from the tunnel walls) is very complex to be accurately depicted theoretically, but can be observed in the measurements and easily reproduced by the empirical model extracted from measured results. Hence, an empirical model is established for the path loss and shadow fading in the near shadowing zone.

- Traditional modal analysis tracks the propagation of every guided wave, but the quantity and type of all the excited modes are normally not involved in the expressions. In the proposed limited multi-mode model for the multi-mode propagation zone and the fundamental mode propagation zone, the quantity and type of all the modes are determined and expressed in the formulas.

- Ray tracing method [14] provides accurate predictions, but with heavy computation and extremely rigorous environment information. Hence, the ray tracing method is not employed for the prediction of the whole cell, but utilized to deduce the mode intensity on the excitation plane in the limited multi-mode model, which improves the traditional modal analysis and well transforms the advantages of ray tracing techniques.

2.1. Propagation Loss in the Free Space Propagation Zone and the Extreme Far Zone

In the adjacent region of Tx, the first Fresnel zone is not large enough to touch any wall of the tunnel. Thus, there is a clear LOS, high attenuation of reflected rays, and neglected diffraction. Finally, the propagation characteristics follow the rule of the free space propagation. Correspondingly, this region is named as the free space propagation zone. Here, the waveguide mechanism, even the multi-mode waveguide mechanism, is not established yet because of the high attenuation of (even the first-order) reflected rays.

Similarly, when the distance between Tx and Rx is extremely far, the waveguide effect, even the basic mode waveguide effect, vanishes because of the attenuation at each reflection. Hence, the path loss slope follows the free space propagation loss curve, with occasional deep fades resulting from a single reflected ray from the walls. This zone is observed in some long tunnels, such as the high-speed railway tunnel in Spain [10] and the road tunnel from Slovenia to Austria [12]. Note that the extreme far zone is not obvious in some cellular communication systems whose radius is shorter than 500 m, as the cell ends before the

distance extends to this zone. However, the extreme far zone cannot be ignored in public protection and disaster relief communications, such as Terrestrial Trunked Radio (TETRA) communication systems. These professional mobile communication systems require the validity of their application at higher distances between Tx and Rx.

The channel loss in the free space propagation zone and the extreme far zone can be modeled by the free space model:

$$L_{R_{FS}} \text{ (dB)} = -10\log_{10}\left[\frac{\lambda^2}{(4\pi)^2|z_r - z_t|^2}\right] \tag{1}$$

where $L_{R_{FS}}$ is the propagation loss in the free space propagation zone; $|z_r - z_t|$ is the distance between Tx and Rx; λ is the wavelength.

2.2. Statistical Modeling in the Near Shadowing Zone

The free space propagation zone is very clear when the users are small in size. For instance, the user is pedestrian or light car. However, in typical realistic vehicular communication cases, such as trains in subway tunnels, this segment can be (partially) replaced by another region: the near shadowing zone, which is discovered in the measurements reported in [13]. The measurements employed a configuration of two antennas, one installed in the front and one in the rear car of the train. It is known that this configuration provides good results, and therefore, it is widely used in reality. Details of the measurements can be found in [13].

As shown in Fig. 2(a), an important phenomenon has been observed: when the train is passing in front of the Tx, the received signal power suffers a deep fading, and the propagation has strong multi-path. We call this phenomenon near shadowing. Note that although the measurement is performed at 2.4 GHz, it still represents the common character of all the real advanced radio communication systems. Since in the real systems, antennas are directive, so it is very difficult to get the LOS with the Tx when the train is passing, even if the antennas are located in the upper part of the train.

By involving the shadow fading and using the point slope form, the loss $L_{R_{NS}}$ in the near shadowing zone is expressed by

$$L_{R_{NS}} = \frac{PL_l - (NL_{\max} + PL_0)}{l_{near}}|z_r - z_t| + (NL_{\max} + PL_0) + X_\sigma \tag{2}$$

where $|z_r - z_t|$ is the distance between Tx and Rx; PL_l represents the path loss at the point where the distance is the length of the train; l_{near} is the half length of the near shadowing zone, always equaling the length of vehicle; PL_0 is the path loss under LOS condition when
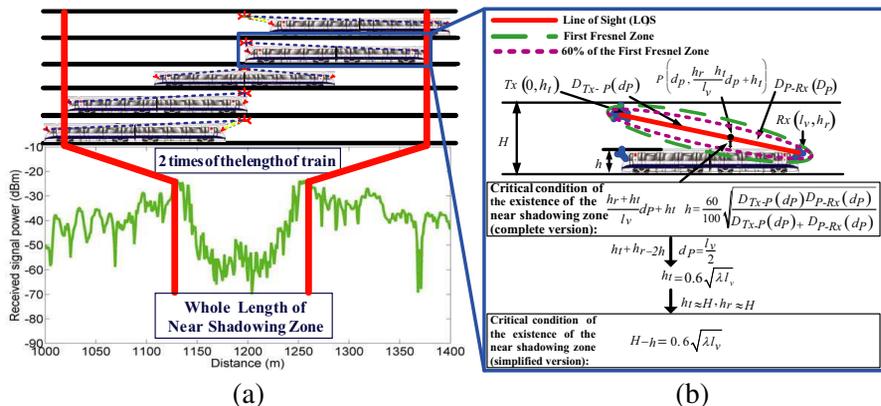
Figure 2. (a) Process of the near shadowing zone and the measured results in [13]; (b) sketch of the mechanism and the critical condition of the near shadowing phenomenon, where H and h denote the height of the tunnel and vehicle, respectively; λ denotes the wavelength; l_v denotes the length of the vehicle.

the distance between Tx and Rx is $0\,\mathrm{m}$, calculated by the free space propagation model. X_σ represents a log-normal distribution with standard deviation σ. $NL_{\max}$ is the maximum near shadowing loss when there is no LOS between Tx and Rx, which is modeled by using the principle of least-squares curve fitting on the measured data in [13]. Details of modeling and parameters can be found in [13, 16].

2.3. Critical Condition of the Near Shadowing Phenomenon and Distinction of Large-size User and Small-size User

The essence of the near shadowing phenomenon is that the first Fresnel zone, especially the 60% of the first Fresnel zone is blocked by the vehicle itself. Hence, as shown in Fig. 2(b), the critical condition of the near shadowing phenomenon can be given when the vertical distance between any point P on the LOS and the top of the vehicle is equal to the 60% of the radius of the first Fresnel zone. When $d_P = \frac{l_v}{2}$, the complete version of the critical condition can be simplified as $h_t + h_r - 2h = 0.6\sqrt{\lambda l_v}$, which indicates that even the widest part of the 60% of the first Fresnel zone is touched by the vehicle. Since the transmitting antenna is normally installed slightly under the top of the tunnel, and the receiving antenna is deployed on the vehicle, the critical condition can be finally simplified to be the relations among the wavelength, the hight of the tunnel, and the hight of the user.

Correspondingly, when $H - h < 0.6\sqrt{\lambda l_v}$ is fulfilled, the user is classified as the large-size user, the near shadowing phenomenon

should be considered in the network planning. Contrarily, when $H - h > 0.6\sqrt{\lambda l_v}$ is met, the user is defined as the small-size user, the near shadowing phenomenon does not exist.

2.4. Limited Multi-mode Modeling in the Multi-mode Propagation Zone and the Fundamental Model Propagation Zone

The traditional multi-mode model presented in [17] is mature but two aspects of knowledge are still absent: the quantity and the type of the modes, and the influence of the tilt and roughness of walls. In this paper, to accurately predict the propagation, a limited multi-mode model is proposed, which complements the missing information of the traditional model. By assuming the arched and circular tunnel approximated to an equivalent rectangular tunnel, the quantity and the type of modes are determined by the frequency and the tunnel:

$$
\begin{aligned}
&m \in [1, m_{\max}], \\
&1 \leq n_{ij} \leq \left\lfloor \frac{H}{W} \sqrt{4W^2 f_0^2 \mu_0 \varepsilon_0 \varepsilon_a - m_i^2} \right\rfloor, \\
&i \in [1, m_{\max}], j \in \left[1, \left\lfloor \frac{H}{W} \sqrt{4W^2 f_0^2 \mu_0 \varepsilon_0 \varepsilon_a - m_i^2} \right\rfloor \right]
\end{aligned}
\tag{3}
$$

where m and n are approximate numbers of half-wave loops in the horizontal and vertical directions. W and H are the width and height of the tunnel; f_0 denotes the central frequency of the signal; ε_0 and ε_a are the permittivity in vacuum space and the relative permittivity for the air in the tunnel, respectively. μ_0 denotes the permeability for vertical/horizontal walls and the air in the tunnel. $m_{\max}$ denotes the maximum of m, which can be given by

$$
m_{\max} = \left\lfloor \frac{W}{H} \sqrt{4H^2 f_0^2 \mu_0 \varepsilon_0 \varepsilon_a - 1} \right\rfloor
\tag{4}
$$

Finally, by introducing two modifying factors (the tilt loss — L_{tilt} and the roughness loss — $L_{roughness}$) [18], the propagation loss $L_{R_{MW}}$ at the coordinate $(x, y, |z_r - z_t|)$ can be analytically calculated:

$$
L_{R_{MW}} = L_{tilt}(|z_r - z_t|) \, [\text{dB}] + L_{roughness}(|z_r - z_t|) \, [\text{dB}]
$$
$$
- 20 \lg \left(\frac{1}{E_0} E^{Rx}(x, y, |z_r - z_t|) \right) - G_t \, [\text{dB}] - G_r \, [\text{dB}]
\tag{5}
$$

where E_0 is the field at the Tx. G_t and G_r are the antenna gains of the Tx and the Rx, respectively. Details can be found in [16].

3. MODELING FOR DIVIDING POINTS BETWEEN DIFFERENT PROPAGATION ZONES

3.1. Modeling for Dividing Point 1

The Dividing Point 1 locates at the distance when the Maximum first Fresnel zone first touches any one of the walls:

$$z_{DV}^{FSZ\text{-}MMZ} = \min \left\{ z_{r\min}^{f_i}, i = 1, 2, \ldots, n \right\} \qquad (6)$$

where $z_{DV}^{FSZ\text{-}MMZ}$ denotes the distance between the Tx and the Dividing Point 1; n is the number of the walls of the tunnel. $z_{r\min}^{f_i}$ denotes the location of the Dividing Point 1 when only the wall $f_i(x, y, z)$ could be touched by the Maximum first Fresnel zone. Details and simplified formulas of the Dividing Point 1 in arbitrary cross-sectional tunnels are given by [19]. This model has been validated by five groups of measurement campaigns conducted in various tunnels in [4, 10, 12, 13]. The tunnels used for validation possess great diversity: the tunnel type includes road tunnel, pedestrian tunnel, and railway tunnel; the cross section involves rectangle, circle, and arch; the operating frequency covers 400 MHz, 450 MHz, and 900 MHz.

3.2. Modeling for Dividing Point 2

Figure 2(a) demonstrates the whole process of the near shadowing phenomenon. The near shadowing phenomenon starts when the distance between train and Tx is shorter than the length of the train and ends when the train is out of this region. Thus, the near shadowing region lasts twice the length of the train (in the measurement [13] is $(2 \times 60 \,\mathrm{m})$). In fact, not only in the train communication, this phenomenon exists when the critical condition is fulfilled. Hence, the Dividing Point 2 between the near shadowing zone and the next zone locates at the distance of the length of the large-size user:

$$z_{DV}^{NSZ\text{-}MMZ} = l_{large\_size\_user} \qquad (7)$$

where $l_{large\_size\_user}$ denotes the length of the large-size user.

3.3. Modeling for Dividing Point 3

Before the Dividing Point 3 and after the Dividing Point 1 (or the Dividing Point 2) is the multi-mode propagation zone, where the high-order modes are significant, and therefore, the signal suffers larger loss. After the Dividing Point 3 and before the Dividing Point 4 is the fundamental mode propagation zone, where the high order modes have

been greatly attenuated so that the signal undergoes smaller loss. By assuming an equivalent rectangular tunnel, the location of the Dividing Point 3 is defined as the distance where the second-fundamental modes have suffered one reflection from (vertical or horizontal) walls. The formulas of the locations of the Dividing Point 3 in equivalent rectangular tunnels and circular tunnels are cited in Fig. 3.
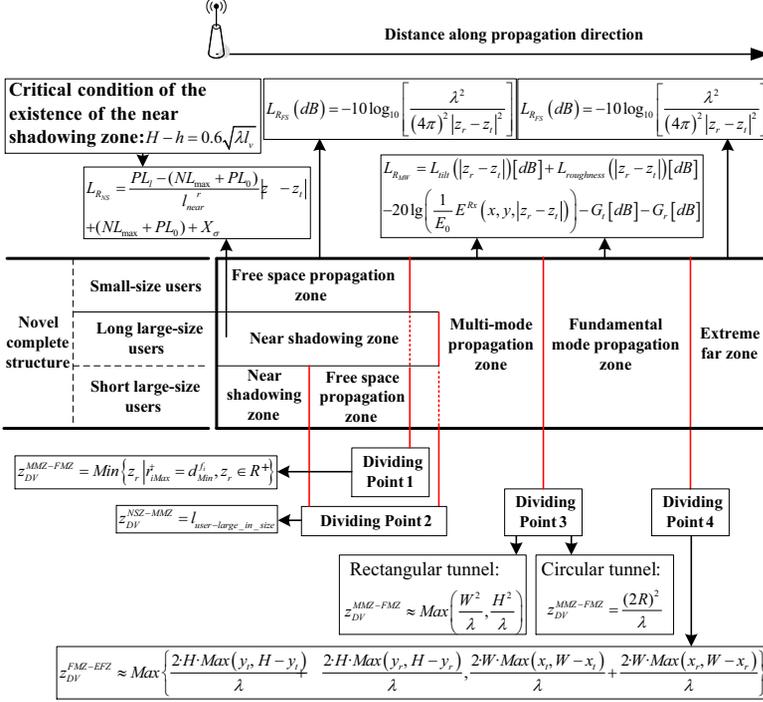
Figure 3. Panorama of the propagation inside tunnels, where the equations can be used to realize a fast and accurate network planning for all types of users inside tunnels.

3.4. Modeling for Dividing Point 4

The Dividing Point 4 indicates the termination of the wave guide mechanism. It locates at the distance where the fundamental modes E_{11}^h (horizontally polarized E-field) and E_{11}^v (vertically polarized E-field) have suffered one reflection [16]. In an equivalent rectangular tunnel, the E_{11}^h mode is defined by the phase relations: $\sin \phi_V = \frac{\lambda}{2W}$; the E_{11}^v mode is defined by the phase relations: $\sin \phi_H = \frac{\lambda}{2H}$, where ϕ_V and ϕ_H are the grazing angles of incidence of the rays with the vertical and horizontal walls, respectively. By using triangular functions and

the approximation: $\tan \phi_V \approx \frac{\lambda}{2W}$, $\tan \phi_H \approx \frac{\lambda}{2H}$, when λ is small compared to W and H, Dividing Point 4 ($z_{DV}^{FMZ\text{-}EFZ}$) locates at:

$$z_{DV}^{FMZ\text{-}EFZ} \approx \max \left\{ \frac{2 \cdot H \cdot \max(y_t, H - y_t)}{\lambda} + \frac{2 \cdot H \cdot \max(y_r, H - y_r)}{\lambda}, \right.$$
$$\left. \frac{2 \cdot W \cdot \max(x_t, W - x_t)}{\lambda} + \frac{2 \cdot W \cdot \max(x_r, W - x_r)}{\lambda} \right\} \quad (8)$$

where x_t and y_t are the horizontal and vertical coordinates of Tx, respectively; x_r and y_r are the corresponding coordinates of Rx.

3.5. Panorama of the Complete Propagation Model Structure inside Tunnels

Figure 3 shows the panorama of the complete propagation model structure. All the propagation losses and the locations of all the dividing pints are analytically modeled. With the equations offered in the panorama, the fast and accurate network planning can be easily realized. Moreover, this panorama includes all the propagation mechanisms and the corresponding constitutions for various types of users, which is very helpful to form a comprehensive understanding of the propagation inside tunnels.

4. SIMULATIONS AND MODEL VALIDATION

In order to validate the proposed model, two groups of measurements in railway and subway tunnels are employed.

4.1. Comparisons with Measurement in Railway Tunnel

The first set of measurements are carried out in the planning of the Global System for Mobile Communication for Railway (GSM-R) of the tunnels on the new high-speed train line from Madrid to Lleida in Spain. Detailed parameters of the measurements can be found in [10].

Figures 4(a) and (b) show the comparisons of the predicted results of the hybrid propagation model and the received signal power in the measurements of the first transmitter (Tx 1) and the second transmitter (Tx 2), respectively. It can be found that the model accurately predicts the attenuation velocity, path loss in the free space propagation zone and the extreme far zone, the small-scale fading in the multi-mode propagation zone, and the flat fading in the fundamental mode propagation zone. Moreover, the dividing points divide the propagation process along the tunnel into four zones. Each zone has its own propagation characteristics and mechanism. It is noted
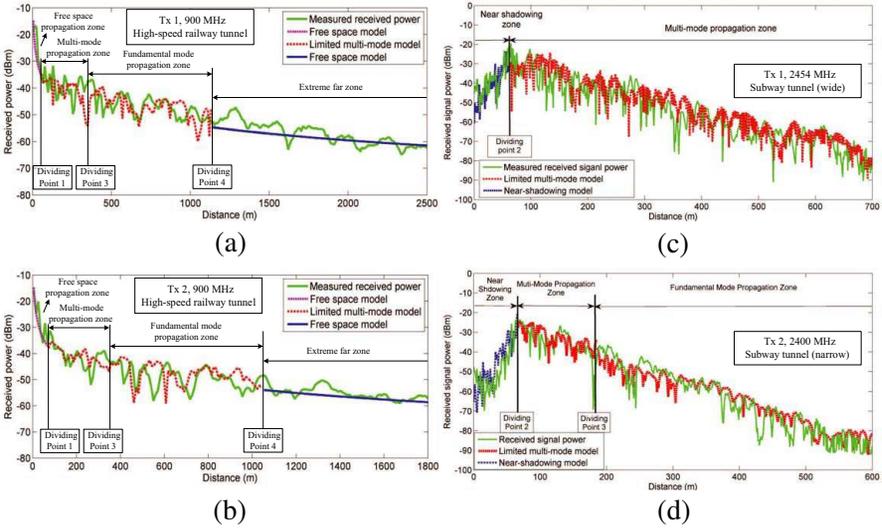
Figure 4. Comparisons between the proposed model and the measurements: (a) Tx 1 and (b) Tx 2 in railway tunnels at 900 MHz; (c) Tx 1 and (d) Tx 2 in subway tunnels at 2.4 GHz.

that the near shadowing zone is not reflected in this case. This is because according to the configurations in [10], $(H - h = 2.8) > (0.6\sqrt{\lambda l_v} = 2.68)$, which means that even though the absolute size of the train is not small, the train in this case (inside this tunnel and with this frequency) do not meet the condition of the large-size user. Thus, the near shadowing zone does not exist in this case, but is replaced by the free space propagation zone.

4.2. Comparisons with Measurement in Subway Tunnel

The second group of measurements are performed at 2.4 GHz, for the planning of the Communication Based Train Control (CBTC) system in the Line 10 tunnels of Madrid's subway, between Tribunal and Príncipe Pio stations. Detailed parameters in the measurements are given by [13].

As shown in Figs. 4(c) and (d), the predicted results and the measured received signal power have good agreement in every propagation zones both for Tx 1 and Tx 2. There are three points worth noting. First, in this case, $(H - h = 0.8) < (0.6\sqrt{\lambda l_v} = 1.64)$. So, the near shadowing zone exists. Second, the free space propagation zone is replaced by the near shadowing zone. Since the length of the near shadowing zone (2 times of the length of the train) is longer than the free space propagation zone in this case, only the near shadowing

zone can be observed before the multi-mode propagation zone. Third, the extreme far zone is not reflected. This is because that the received power at 2.4 GHz is lower than the demodulation threshold before the distance extends to the extreme far zone.

The mean (Mean Error), standard deviation (Std), and root mean square (RMSE) of the difference between the measurements and the proposed model are summarized in Table 2. The proposed model has the ME between 0.1–1.5 dB and the RMSE smaller than 7 dB.

Table 2. Mean, standard deviation, and root mean square of the difference (measurement VS. proposed propagation model).

Tunnel	Railway tunnel		Subway tunnel	
Frequency	900 MHz		2.4 GHz	
System	GSM-R		CBTC	
Tx	Tx 1	Tx 2	Tx 1	Tx 2
ME [dB]	0.9	0.1	0.6	1.5
Std [dB]	3.8	3.8	6.9	6.2
RMSE [dB]	3.9	3.8	6.9	6.4

4.3. Discussions on Complete Model Structure and Segmentation-based Modeling Thought

Based on the modeling, measurements, and simulations, the research on the structure analysis based on the segmentation-based modeling thought leads the following discussions:

- Single modeling technique is always sensitive to certain propagation mechanisms. Since the propagation inside tunnels includes various mechanisms, the segmentation-based thought that divides the whole process into different segments and employs proper techniques in each region supplies an easy and effective way to model the propagation inside tunnels.

- Since the basic philosophy of the segmentation-based modeling thought is to describe the propagation characteristics according to the mechanism in each zone. Hence, the accurate degree of revealing various propagation mechanisms and dividing corresponding zones is the key of this kind of models. The structure of the segmentation proposed in this paper covers five propagation mechanisms and gives heuristic explanations on every region. This renders it more accurate, complete, and comprehensive than previous model structures.

- The propagation models in different zones emphasize various propagation characteristics. The model in the free space

propagation zone and the extreme far zone predicts the path loss; the model in the near shadowing zone describes both the path loss and the shadow fading; the model in the multi-mode propagation zone and the fundamental mode propagation zone reveals the sum of the path loss, the shadowing fading, and the small-scale fading. These propagation models are based on different modeling techniques, so that it gives the chance to make the most of the advantages of various modeling methods. Since there is an interaction between the path loss curves in different zones, the continuity of the predicted path loss can be ensured in the transition between every two zones.

- The dividing points between any two zones are significant as well. Without precise prediction of the location of every dividing point, the segmentation-based model cannot work. In the novel structure, four dividing points are ascertained. The Dividing Point 1 is analytically modeled by conjunctively using the propagation theory and the three-dimensional solid geometry. The Dividing Point 2 is empirically modeled by the measured results. The Dividing Point 3 and the Dividing Point 4 are analytically modeled by employing the GO model and the waveguide model.

- Even though a hybrid model is proposed to characterize the propagation in every zone, it does not mean that the model in this paper is unique or always the best solution. There are still some chances to employ other models according to different requirements of concrete situations. For instance, if only the path loss is required, the models in [10] can also be utilized in the multi-mode propagation zone and the fundamental mode propagation zone. These models do not involve the fading information, but are easier than the limited multi-mode model.

5. CONCLUSION

This paper presents a complete model structure consisting of five propagation zones, four dividing points, and three propagation constitutions, for two types of users. This structure covers all the propagation mechanisms and corresponding zones inside tunnels, refining and extending previous segmentation-based models. Compared with the traditional structure of two regions and the advanced structure of four segments, the novel one subdivides the near region into two zones, which renders the model more accurate in the previous so-called the near region. Moreover, the complete structure adds the extreme far zone and the near shadowing zone, which makes the model more comprehensive. Last but not least, the new structure

gives the analytical solutions for the dividing points inside arbitrary cross-sectional tunnels, which lets the model more general. Validations show that the novel model structure can be flexibly used for various concrete situations, such as the design of the radio communication systems in realistic road tunnels, subway tunnels, and railway tunnels.

ACKNOWLEDGMENT

REFERENCES

1. Bernardi, P., D. Caratelli, R. Cicchetti, V. Schena, and O. Testa, "A numerical scheme for the solution of the vector parabolic equation governing the radio wave propagation in straight and curved rectangular tunnels," *IEEE Trans. on Antennas Propag.*, Vol. 57, 3249–3257, 2009.

2. Phaebua, K., C. Phongcharoenpanich, M. Krairiksh, and T. Lertwiriyaprapa, "Path-loss prediction of radio wave propagation in an orchard by using modified UTD method," *Progress In Electromagnetics Research*, Vol. 128, 347–363, 2012.

3. Liu, Z.-Y. and L.-X. Guo, "A quasi three-dimensional ray tracing method based on the virtual source tree in urban microcellular environments," *Progress In Electromagnetics Research*, Vol. 118, 397–414, 2011.

4. Dudley, D. G., M. Lienar, S. F. Mahmud, and P. Degauque, "Wireless propagation in tunnels," *IEEE Antennas Propag. Magazine*, Vol. 49, 11–26, 2007.

5. Sanchez-Escuderos, D., M. Ferrando-Bataller, J. I. Herranz, and M. Baquero-Escudero, "Optimization of the E-plane loaded rectangular waveguide for low-loss propagation," *Progress In Electromagnetics Research*, Vol. 135, 411–433, 2013.

6. Dong, J.-F. and J. Li, "Characteristics of guided modes in uniaxial chiral circular waveguides," *Progress In Electromagnetics Research*, Vol. 124, 331–345, 2012.

7. Vaccari, A., A. Cala' Lesina, L. Cristoforetti, and R. Pontalti, "Parallel implementation of a 3D subgridding FDTD algorithm for large simulations," *Progress In Electromagnetics Research*, Vol. 120, 263–292, 2011.

8. Lee, Y.-G., "Electric field discontinuity-considered effective-permittivities and integration-tensors for the three-dimensional finite-difference time-domain method," *Progress In Electromagnetics Research*, Vol. 118, 335–354, 2011.

9. Izadi, M., M. Z. A. Ab Kadir, and C. Gomes, "Evaluation of electromagnetic fields associated with inclined lightning channel using second order FDTD-hybrid methods," *Progress In Electromagnetics Research*, Vol. 117, 209–236, 2011.

10. Briso-Rodriguez C., J. M. Cruz, and J. I. Alonso, "Measurements and modeling of distributed antenna systems in railway tunnels," *IEEE Trans. on Veh. Technol.*, Vol. 56, 2870–2879, 2007.

11. Zhang, Y. P., "Novel model for propagation loss prediction in tunnels," *IEEE Trans. on Veh. Technol.*, Vol. 52, 1308–1314, 2003.

12. Hrovat, A., G. Kandus, and T. Javornik, "Four-slope channel model for path loss prediction in tunnels at $400\,\mathrm{MHz}$," *IET Microwaves, Antennas and Propagation*, Vol. 4, 571–582, 2010.

13. Guan K., Z. D. Zhong, B. Ai, C. Briso, and J. I. Alonso, "Measurement of distributed antenna systems at $2.4\,\mathrm{GHz}$ in a realistic subway tunnel environment," *IEEE Trans. on Veh. Technol.*, Vol. 61, 834–837, 2012.

14. Song, X. and R. Leonhardt, "Ray-optics analysis of single mode condition for optical waveguides with rectangular cross-section," *Progress In Electromagnetics Research*, Vol. 135, 81–89, 2013.

15. Zhang, Y., W. Zhai, X. Zhang, X. Shi, X. Gu, and Y. Deng, "Ground moving train imaging by Ku-band radar with two receiving channels," *Progress In Electromagnetics Research*, Vol. 130, 493–512, 2012.

16. Guan, K., Z. Zhong, B. Ai, R. He, and C. Briso-Rodriguez, "Five-zone propagation model for large-size vehicles inside tunnels," *Progress In Electromagnetics Research*, Vol. 138, 389–405, 2013.

17. Sun, Z. and I. F. Akyildiz, "Channel Modeling and analysis for wireless networks in underground mines and road tunnels," *IEEE Trans. on Communications*, Vol. 58, No. 6, 1758–1768, 2010.

18. Emslie, A. G., R. L. Lagace, and P. F. Strong, "Theory of the propagation of uhf radio waves in coal mine tunnels," *IEEE Trans. on Antennas Propag.*, Vol.23, No. 2, 192–205, 1975.

19. Guan, K., Z. Zhong, B. Ai, R. He, Y. Li, and C. Briso, "Propagation mechanism modeling in the near-region of arbitrary cross-sectional tunnels," *International Journal of Antennas and Propagation*, Vol. 2012, Article ID 183145, 11 Pages, 2012, doi:10.1155/2012/183145.